

# Attentive Relational Networks for Mapping Images to Scene Graphs

Mengshi Qi<sup>\*1</sup>, Weijian Li<sup>\*2</sup>, Zhengyuan Yang<sup>2</sup>, Yunhong Wang<sup>1</sup>, and Jiebo Luo<sup>2</sup>

<sup>1</sup>Beijing Advanced Innovation Center for Big Data and Brain Computing, School of Computer Science and Engineering, Beihang University, China

<sup>2</sup>Department of Computer Science, University of Rochester, USA

{qi\_mengshi, yhwang}@buaa.edu.cn, {wli69, zyang39, jluo}@cs.rochester.edu

## Abstract

Scene graph generation refers to the task of automatically mapping an image into a semantic structural graph, which requires correctly labeling each extracted objects and their interaction relationships. Despite the recent successes in object detection using deep learning techniques, inferring complex contextual relationships and structured graph representations from visual data remains a challenging topic. In this study, we propose a novel Attentive Relational Network that consists of two key modules with an object detection backbone to approach this problem. The first module is a semantic transformation module used to capture semantic embedded relation features, by translating visual features and linguistic features into a common semantic space. The other module is a graph self-attention module introduced to embed a joint graph representation through assigning various importance weights to neighboring nodes. Finally, accurate scene graphs are produced with the relation inference module by recognizing all entities and the corresponding relations. We evaluate our proposed method on the widely-adopted Visual Genome Dataset, and the results demonstrate the effectiveness and superiority of our model.

## 1. Introduction

Visual Scene understanding [10, 46, 14] is a fundamental problem in computer vision. It aims at capturing the structural information in an image including the object entities and pair-wise relationships. As shown in Figure 1, each entity and relation should be processed with a broader context to correctly understand the image at semantic level. During recent years, deep neural network based object detection models such as Faster-RCNN [29] and YOLO [28]

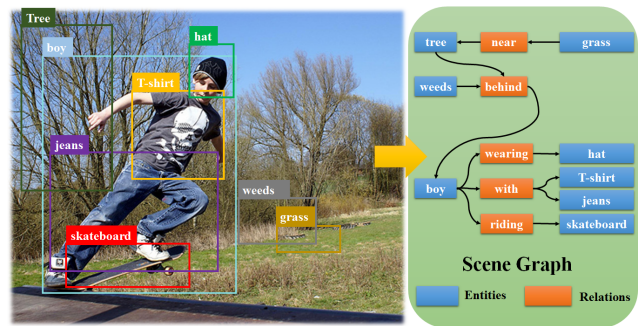


Figure 1. Illustration of the task of scene graph generation. Using our proposed Attentive Relational Network, an image can be mapped to a scene graph, which captures individual entities (e.g. boy, tree and grass) and their relationships (e.g. <boy-riding-skateboard> and <weeds-behind-boy>).

have achieved a great improvement. However, such conventional object detection approaches cannot capture and infer the relationships within an image. The highly diverse visual appearances and the large numbers of distinct visual relations make scene graph generation a challenging task.

Because of its ability to enrich semantic analysis and clearly describe how objects interact with each other (e.g. ‘a boy is riding a skateboard’ in Figure 1), generating accurate scene graphs from images plays a significant role in multiple computer vision applications such as image retrieval [10, 26], image captioning [17, 38], visual question answering [15, 32] and video analysis [25].

Previous scene graph generation methods [35, 41, 8, 17, 20, 36, 16] locate and infer the visual relationship as a triplet in the form <subject-predicate-object>, and the predicate is a preposition word used to link a pair of objects, e.g. <boy-wearing-hat> in Figure 1. There exist various kinds of relationships happened between two objects, including spatial positions (e.g. under, above), attributes/prepositions (e.g. with, of), comparatives (e.g. taller, fatter) and actions/ verb (e.g. play, ride). Most of the existing

<sup>\*</sup>Equal contribution.

works neglect the semantic relationship between the visual feature and linguistic knowledge, and the intrinsic connection among the triplet.

Moreover, previous works invariably utilize conventional deep learning models such as Convolutional Neural Networks (CNN) [17, 20, 36, 16] or Recurrent Neural Networks [35, 41, 8] for scene graph generation. These methods require to know the graph structure beforehand and contain computationally intensive matrix operations during approximation. Moreover, most of them follow a step-by-step manner to capture the representation of nodes and edges, leading to neglect of the global structure and information in whole image. Effectively extracting a whole joint graph representation to model entire scene graph for reasoning is promising but remains an arduous problem.

To address the aforementioned issues, we propose a novel *Attentive Relational Network* that maps images to scene graphs. To be specific, the proposed method first adopts an Object Detection Module to extract the localization and category probability of each entity and relation. Then a semantic transformation module is introduced to translate entities and relation features as well as their linguistic representation into a common semantic space. In addition, we present a graph self-attention module to jointly embed an adaptive graph representation through measuring the importance of the relationship between neighboring nodes. Finally, a relation inference module is presented to classify each entity and relation by a Multi-layer Perceptron (MLP), and generates an accurate scene graph.

Our main contributions are summarized as follows:

- A novel Attentive Relational Network is proposed for scene graph generation, which translates visual information to a graph-structured representation.
- A semantic transformation module is designed to incorporate relation features with entity features and linguistic knowledge, by simultaneously transforming word embedding and visual features into a common semantic space.
- A graph self-attention module is introduced to jointly embed the whole graph representation by implicitly specifying different weights to different neighboring nodes. To our best knowledge, this is the first attempt to introduce self-attention mechanism in this task.
- Extensive experiments on the *Visual Genome Dataset* comprehensively verify the superior performance of the proposed method compared to the state-of-the-art methods.

## 2. Related Work

**Scene Graph Generation** A mass of efforts have been devoted to this issue during recent years, which can

be divided into two categories: Recurrent Neural Networks (RNN)-based methods [35, 41, 8] and Convolutional Neural Networks (CNN)-based approaches [17, 20, 36, 16]. Xu *et al.* [35] employ RNNs to infer scene graphs by message passing. Zellers *et al.* [41] introduce *motifs* to capture the common substructures in scene graphs. To minimize the effect of different input factors' order, Herzig *et al.* [8] propose a permutation invariant structure prediction model. Li *et al.* [17] construct a dynamic graph to address object detection, scene graph generation and region captioning jointly. To overcome the weakness of object detection-based methods, Newell *et al.* [20] present associative embedding [21] for predicting graphs from pixels. Yang *et al.* [36] propose a Graph R-CNN for selecting the important object bounding boxes pairs and utilize graph convolutional network [11] for structure embedding. Li *et al.* [16] present a Factorizable Net to capture subgraph-based representations. Different from these previous work, our proposed Attentive Relational Network focuses on semantic relations which includes a semantic transformation module to jointly embed linguistic knowledge and visual representations.

**Visual Relationship Detection** Early efforts in visual relationship detection [2, 5, 27, 30] tend to adopt a joint model regarding the relation triplet as a unique class. Among these work, Lu *et al.* [19] utilize relationship embedding space from the language and object appearance model for visual relationship prediction. The visual embedding network [42, 40, 47] places objects in a low-dimensional relation space and integrates extra knowledge. However, these works can not learn intrinsic semantic knowledge for graph representation embedding. Plummer *et al.* [24] combine different cues with learning weights for grounded phrase. Liang *et al.* [18] adopt variation-structured reinforcement learning to sequentially discover object relationships. Dai *et al.* [4] exploit the statistical dependencies between objects and their relationships. Recently, various studies [45, 43, 23, 15, 37, 39, 9, 12, 44] propose relationship proposal networks by employing pairwise regions in images for fully or weakly supervised visual relation detection. However, most of them are designed for detecting relationship one-by-one, which is inappropriate for describing the structure of the whole scene graph. Our proposed graph self-attention module in our model aims at embedding a joint graph representation to describe all relationships occurred in an image, and applying it for scene graph generation.

## 3. Proposed Approach

### 3.1. Overview

**Problem Definition:** We define the *scene graph* of an image  $I$  as  $G$ , which describes the category of each entity and semantic inter-object relationships. A set of entity

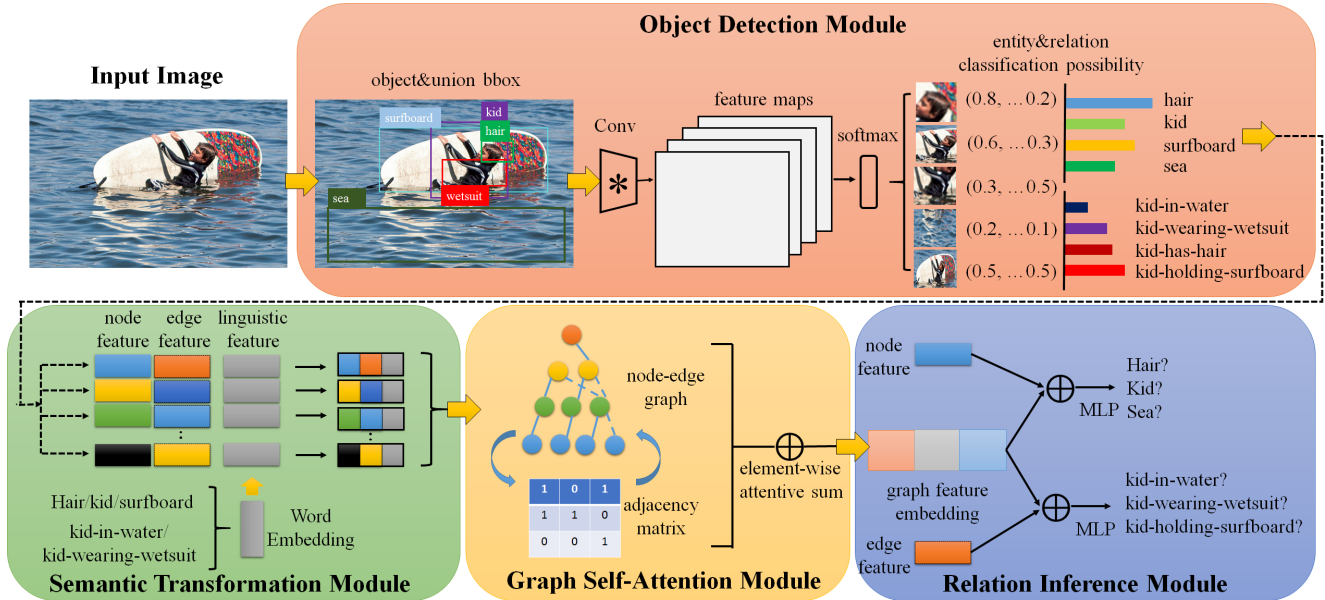


Figure 2. Overview of the proposed Attentive Relational Network. Our model mainly consists of four parts: (1) *Object Detection Module*: capturing the visual feature and the location of each entity bounding box with their pair-wise relation bounding boxes. Then a softmax function is employed to obtain initial classification scores for each entity and relation; (2) *Semantic Transformation Module*: producing the semantic embedded representations by transforming label word embeddings and visual features into a common semantic space; (3) *Graph Self-Attention Module*: leveraging a self-attention mechanism to embed entities via constructing an adjacency matrix based on the space position of nodes; (4) *Relation Inference Module*: creating the joint global graph representation and predicting entity and relationship labels as final scene graph result.

bounding boxes as  $B = \{b_1, \dots, b_n\}$ ,  $b_i \in \mathbb{R}^4$  and their corresponding class label set  $O = \{o_1, \dots, o_n\}$ ,  $o_i \in C$ , where  $C$  is object categories set. The set of binary relationships between objects are referred to as  $R = \{r_1, \dots, r_m\}$ . Each relationship  $r_k \in \mathbb{R}$  is a triplet in a <subject-predictive-object> format, where a subject node  $(b_i, o_i) \in B \times O$ , a relationship label  $l_{ij} \in \mathbb{R}$  and an object node  $(b_j, o_j) \in B \times O$ .  $\mathbb{R}$  is the set of all predicate category set<sup>1</sup>.

**Graph Inference:** Each Scene graph comprises of a collection of bounding boxes  $B$ , entity labels  $O$  and relation labels  $R$ . The possibility of inferring a scene graph from an image can be formulated as the following:

$$Pr(G|I) = Pr(B|I)Pr(O|B, I)Pr(R|B, O, I). \quad (1)$$

The formulation can be regarded as the factorization without independence assumptions. The  $Pr(B|I)$  can be inferred by object detection module in our model described in 3.2, while  $Pr(O|B, I)$  and  $Pr(R|B, O, I)$  can be inferred by the rest modules proposed in our model.

Figure 2 presents the overview of our proposed Attentive Relational Network, which contains four modules, namely object detection module, semantic transformation module, graph self-attention module and relation inference module.

<sup>1</sup>We also adding extra ‘bg’ referred to ‘background’, denoting there is no relationship or edge between objects

Our model is aim at producing a joint global graph representation for the image, which contains the whole semantic relation embedded representation learned in semantic transformation module, and the whole entity embedded representation learned in graph self-attention module. Finally, we combine the learned global graph representation and entity/relation feature for problem inference in relation inference module. Next we will introduce the four proposed modules in detail.

### 3.2. Object Detection Module

We employ Faster-RCNN [29] with VGG-16 [31] as our object detector. Then a set of predictable entity proposal  $B = \{b_1, \dots, b_n\}$  from each input image  $I$ , including their locations and appearance features, are obtained. In order to represent the contextual information for visual relation, we generate an union bounding box to cover objects pair with a small margin and extract features via a CNN. Two types of feature representations are adopted for describing entities and relations, *i.e.* the appearance feature and spatial feature. Finally, we employ the softmax function to recognize the category of each entity and relation, and obtain their corresponding classification confidence scores as the initial input to the following modules.

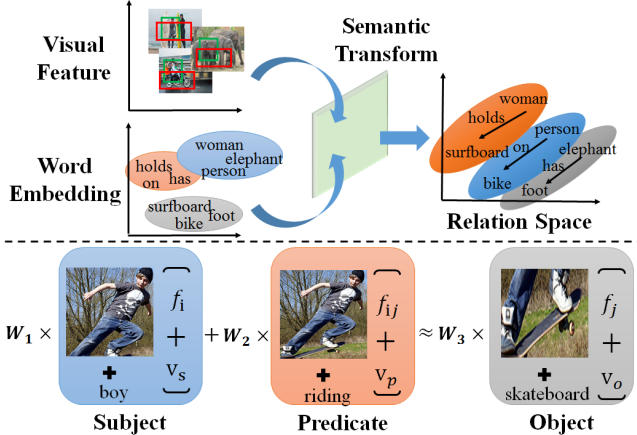


Figure 3. Illustration of Semantic Transformation Module. (Top): Mapping visual feature and word embedding to a common semantic space, and inferring their relationship in the relation space. (Bottom): An example of relation translation. Concatenating the visual features of entities and relation (*i.e.*  $f_i$ ,  $f_j$  and  $f_{ij}$ ) and their corresponding label embedding features (*i.e.* 'boy', 'riding' and 'skateboard':  $v_s$ ,  $v_p$  and  $v_o$ ), and translating them based on <subject-predicate-object> template via learned weight matrices (*i.e.*  $W_1$ ,  $W_2$  and  $W_3$ ).

### 3.3. Semantic Transformation Module

Inspired by Translation Embedding (TransE) [3, 42] and visual-semantic embedding [6], we introduce a semantic transformation module to effectively represent <subject-predicate-object> in the semantic domain. As depicted in Figure 3, the proposed module leverages both visual features and textual word features to learn the semantic relationship between pair-wise entities. It then explicitly maps them into a common relation space. For any relation, we define  $v_s$ ,  $v_p$  and  $v_o$  to represent the word embedding vectors of category labels for *subject*, *predicate* and *object*. To generate specific word embedding vectors for subject, predicates and object, label scores obtained from Object Detection Module and word embedding of all labels are combined with element-wise multiplication. In computational linguistic area, it is known that a valid semantic relation can be expressed as the following [22]:

$$v_s + v_p \approx v_o, \quad (2)$$

Similarly, we assume such a semantic relation exists among the corresponding visual features:

$$f_i + f_{ij} \approx f_j, \quad (3)$$

where  $f_i$ ,  $f_j$  and  $f_{ij}$  are defined as the visual representations of entity  $b_i$ ,  $b_j$  and their relation  $r_{ij}$ , respectively.

It is worth noting that the visual feature and word embedding should be projected into a common semantic space. Hence, we adopt a linear model with three learnable weights

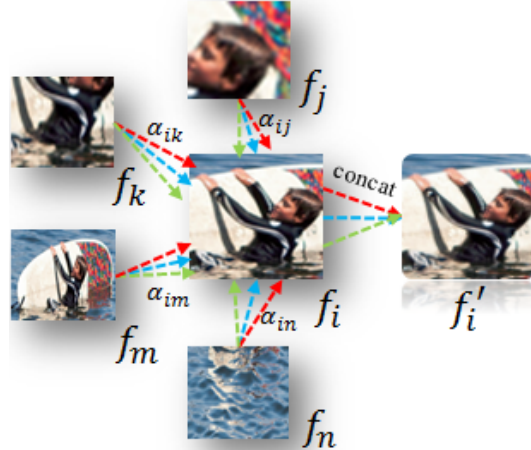


Figure 4. Illustration of graph self-attention module for each single node. The output feature of the  $i$ -th node can be calculated based on its neighboring nodes' features  $f_j$ ,  $f_k$ ,  $f_m$  and  $f_n$  with their corresponding pair-wise attention weight  $\alpha$ . Different color arrows refer to independent attention computations as multi-head attention (*e.g.*  $k=3$  in this figure). The aggregated attentive feature of node  $i$  is denoted as  $f'_i$  via concatenation operation.

to jointly approximate Eq. (2) and Eq. (3). L2 loss is used to guide the learning process:

$$\mathbb{L}_{semantic} = \|W_3 \cdot [f_j, v_o] - (W_1 \cdot [f_i, v_s] + W_2 \cdot [f_{ij}, v_p])\|_2^2, \quad (4)$$

where  $W_1$ ,  $W_2$  and  $W_3$  refer to the weights respectively, and  $[\cdot]$  denotes the concatenation operation. These learned weight matrices can be regarded as the semantic knowledge in relation space.

Then we need to map the visual features of detected entities (*i.e.* nodes) and relations (*i.e.* edges) with such linguistic knowledge into a common semantic domain. The semantic transformed representation of relation  $f_{ij}$  in the scene graph can be denoted as  $\Theta(f_{ij})$ :

$$\Theta(f_{ij}) = (W_1 \cdot [f_i, v_s]) \oplus (W_2 \cdot [f_{ij}, v_p]) \oplus (W_3 \cdot [f_j, v_o]), \quad (5)$$

where  $\oplus$  and  $[\cdot]$  both represent concatenation operation. Finally, we can obtain each semantic relation embedded representation in an image.

### 3.4. Graph Self-Attention Module

The attention mechanism maps the input to a weighted representation over the values. Self-attention has been demonstrated to be effective in computing representations of a single sequence [33, 34]. To compute a relational representation of a single node sequence, we introduce a graph self-attention module that takes both node representations and their neighborhood representations into consideration. By adopting the self-attention mechanism, each node's hidden representation can be extracted by attending over its neighbors and simultaneously preserve the structural relationship.

As shown in Figure 4, we define a collection of input node (entity) features  $F_{node} = \{f_1, f_2, \dots, f_N\}$ ,  $f_i \in \mathbb{R}^M$ , and their corresponding output features  $F'_{node} = \{f'_1, f'_2, \dots, f'_N\}$ ,  $f'_i \in \mathbb{R}^{M'}$ , where  $N$ ,  $M$  and  $M'$  are the number of nodes, input feature dimension and output feature dimension respectively. The attention coefficients  $e_{ij}$  can be performed to denote the importance of node  $j$  to node  $i$ :

$$e_{ij} = \Lambda(U \cdot f_i, U \cdot f_j), \quad (6)$$

where  $\Lambda$  denotes attention weight vector implemented with a single feed-forward layer,  $\Lambda \in \mathbb{R}^{F'} \times \mathbb{R}^{F'} \rightarrow \mathbb{R}^{2F'}$ .  $U \in \mathbb{R}^{M' \times M}$  refers to learnable parameter weight.

We compute the  $e_{ij}$  for each neighboring node  $j \in \mathbb{N}_i$ , where  $\mathbb{N}_i$  denotes the neighboring set of node  $i$ . Then we normalize the coefficients across all neighboring nodes by the softmax function for effective comparable with different nodes:

$$\alpha_{ij} = \text{softmax}_j(e_{ij}) = \frac{\exp(e_{ij})}{\sum_{k \in \mathbb{N}_i} \exp(e_{ik})}. \quad (7)$$

Therefore the coefficients computed can be formulated as:

$$\alpha_{ij} = \frac{\exp(\sigma(\Lambda^T[U \cdot f_i, U \cdot f_j]))}{\sum_{k \in \mathbb{N}_i} \exp(\sigma(\Lambda^T[U \cdot f_i, U \cdot f_k]))}, \quad (8)$$

where  $\sigma$  and  $[\cdot]$  represent LeakyReLU nonlinear activation and concatenation operation. Final node representation is then obtained by applying the attention weights on neighboring node features. Inspired by [33], we employ multi-head attention to capture different aspect relationships from neighboring nodes. The overall output of the  $i$ -th node is a concatenated feature through  $K$  independent attention heads, denoted as  $\Phi(f_i)$ :

$$\Phi(f_i) = \text{Concat}_{k=1}^K \sigma\left(\sum_{j \in \mathbb{N}_i} \alpha_{ij}^k U^k f_j\right), \quad (9)$$

where  $\alpha_{ij}^k$  are normalized attention coefficients by the  $k$ -th attention mechanism, and  $U^k$  is the corresponding input linear transformation's weight matrix<sup>2</sup>.

**Setting of Adjacent Matrix:** In order to compute adjacent matrices, we design four strategies to determine node neighbors based on spacial clues. Concretely, given two bounding boxes  $b_i$  and  $b_j$  as two nodes, their normalized coordinates of locations can be denoted as  $(x_i, y_i)$  and  $(x_j, y_j)$ , and their distance can be denoted as  $d_{ij} = \sqrt{(x_j - x_i)^2 + (y_j - y_i)^2}$ . Then four neighbor classification settings are: (1) Inside Neighbor: if  $b_i$  completely includes  $b_j$ ; (2) Cover Neighbor: if  $b_i$  is fully covered by  $b_j$ ; (3) Overlap Neighbor: if the IoU between  $b_i$  and  $b_j$  is larger than 0.5; (4) Relative Neighbor: if the ratio between the relative distance  $d_{ij}$  and the diagonal length of the whole images is less than 0.5.

<sup>2</sup>In our experiments, we set  $k=8$  following [33].

### 3.5. Relation Inference Module

After obtaining the whole relation embedded representation and entity embedded representation based on Eq. (5) and Eq. (9) respectively, we can construct a global scene graph representation denoted as  $\Omega(G)$ :

$$\Omega(G) = \sum_{i=1}^n \Phi(f_i), \quad (10)$$

$$\text{where } \Phi(f_i) = f_i \oplus \sum_{j \neq i} \Theta(f_{ij}),$$

where  $n$  refers to the number of entities in the image, and  $\sum$  and  $\oplus$  denote element-wise sum and concatenation operation. Then we perform recognition of entity and relation with three layers MLP as the following:

$$\begin{aligned} o'_i &= \text{MLP}(f_i \oplus \Omega(G)), \\ l'_{ij} &= \text{MLP}(f_{ij} \oplus \Omega(G)), \end{aligned} \quad (11)$$

where  $o'$  and  $l'$  refer to the predicted label of entity and relation, respectively. We adopt two cross-entropy loss functions in this module, and define  $o$  and  $l$  as the ground truth label for entity and relation, respectively:

$$\begin{aligned} \mathbb{L}_{entity} &= - \sum_i o'_i \log(o_i), \\ \mathbb{L}_{relation} &= - \sum_i \sum_{j \neq i} l'_{ij} \log(l_{ij}). \end{aligned} \quad (12)$$

In summary, the joint objective loss function in our Attentive Relational Network can be formulated as follows:

$$\mathbb{L} = \lambda_1 \mathbb{L}_{entity} + \lambda_2 \mathbb{L}_{relation} + \lambda_3 \mathbb{L}_{semantic} + \|\mathbb{W}\|_2^2, \quad (13)$$

where  $\lambda_1$ ,  $\lambda_2$  and  $\lambda_3$  denote hyper-parameters to tune the function, and  $\mathbb{W}$  refers to all learned weights in our model.

## 4. Experimental Results

To validate our proposed model, extensive experiments are conducted on the widely-adopted public **Visual Genome (VG) Dataset** [13]. In the following paragraphs, the Visual Genome dataset as well as the implementation details are firstly introduced. Then experimental results and detailed quantitative and qualitative analysis are presented.

### 4.1. Experimental Settings

**Visual Genome (VG) Dataset** [13] includes 108,077 images annotated with bounding boxes, entities and relationships annotated with an open vocabulary. There are 75,729 unique object categories, and 40,480 unique relationship predicates in total. Considering the effect of long-tail distribution, we choose the most frequent 150 object

Table 1. Comparison results of our model and existing state-of-the-art methods on constrained scene graph classification (SGCls) and predicate classification (PredCls) on Visual Genome (VG) [13] test set. **Ours w/ GSA**, **Ours w/ ST** and **Ours-Full** denote our model only with Graph Self-Attention Module, our model only with Semantic Transformation Module and our full model, respectively. The best performances are in bold.

Dataset	Model	SGCls		PredCls	
		Recall@50	Recall@100	Recall@50	Recall@100
VG	LP [19]	11.8	14.1	27.9	35.0
	Message Passing [35]	21.7	24.4	44.8	53.0
	Graph R-CNN [36]	29.6	31.6	54.2	59.1
	Pixel2Graph [20]	26.5	30.0	N/A	N/A
	Neural Motif [41]	35.8	36.5	55.8	58.3
	GPI [8]	36.5	38.8	56.3	60.7
	<b>Ours w/ GSA</b>	37.2	39.4	54.8	59.9
	<b>Ours w/ ST</b>	37.3	40.1	55.2	60.9
	<b>Ours-Full</b>	<b>38.2</b>	<b>40.4</b>	<b>56.6</b>	<b>61.3</b>

categories and 50 predicates for evaluation [35, 20, 41]. Averagely, the scene graph of each image contains about 12 objects and 7 relationships. For fair comparison with previous works, we follow the experimental setting in [35], and split the dataset into 70K/5K/32K for train/validation/test sets.

**Metrics:** Following [1, 19], we adopt the image-wise recall@100 and recall@50 as our evaluation metrics. Recall@X is used to compute the fraction of occurring times the correct relationship is predicted in the top  $x$  confident predictions. The rank strategy is based on confidence scores of object detector and the selected predicates. Meanwhile, we do not choose  $mAP$  as a metric that is a pessimistic evaluation metric, because we can not exhaustively annotate all possible relationships or attributes in an image, and some true relationships may be missing, as discussed in [19]. Besides, we also report per-type recall@5 of classifying individual predicate.

**Task Settings:** In this work, our goal is to infer the scene graph of an image given the confidence scores of entities and relations, while the object detection is not our main objective. Therefore, we conduct two sub-tasks of scene graph generation to evaluate our proposed method following [35, 8]. **(1)Scene Graph Classification (SGCls):** Given ground-truth bounding boxes of entities, the goal is to predict the category of all entities and relations in an image. This task needs to correctly detect the triplet of <subject-predicate-object>. **(2)Predicate Classification (PredCls):** Given a set of ground truth entity bounding boxes with their corresponding localization and categories, the goal is to predict all relations between entities. In all of our experiments, we perform graph-constrained evaluation, which means the returned triplets must be consistent with a scene graph.

**Compared Methods:** We compare our proposed approach with the following methods on the VG: Language

Prior (LP) [19], Iterative Message Passing (IMP) [35], Pixel2Graph [20], Neural Motif [41], Graph R-CNN [36], GPI [8]. In all the experiments, the parameter settings of the above-mentioned methods are adopted from the corresponding papers. Note that some of previous methods use slightly different pre-training procedures or data split or extra supervisions. For a fair comparison, we re-train Neural Motif and GPI with their released codes for evaluation, and ensure all the methods are based on the same backbone.

## 4.2. Implementation Details

We implement our model based on TensorFlow [7] framework on a single NVIDIA 1080 Ti GPU. Similar to prior work in scene graph generation [35, 17], we adopt Faster RCNN (with ImageNet pretrained VGG16) [29] as backbone in our object detection module. Following [41, 17, 35], we adopt two-stage training, where the object detection module is pre-trained for capturing label category possibility as our high-level feature. Furthermore, the Semantic Transformation Module is implemented as three 300-size layers for semantic projection, and one fully-connected (FC) layers for feature embedding that output a vector of size 500, and the word vectors were learned from the text data of Visual Genome with Glove [22]; the Graph Self-Attention Module is implemented by one FC layer that outputs a vector of size 500, and we set  $k = 8$  in Eq. (9) as multi-head attention; the Relation Inference Module is implemented as three FC layers of size 500 and outputs an entity probability vector of size 150 and relation probability vector of size 51 corresponding to the semantic labels in the datasets. We perform an end-to-end training by employing Adam as the optimizer with initial learning rate of  $1 \times 10^{-4}$ , and the exponential decay rate for the 1st and 2nd moment estimates are set as 0.9 and 0.999, respectively. We adopt a mini-batch training with batch size 20.

Table 2. Predicate classification recall of our full model on the test set of Visual Genome. Top 20 most frequent types are shown. The evaluation metric is recall@5.

predicate	ours	predicate	ours
on	98.54	sitting on	80.89
has	98.18	between	78.62
of	96.17	under	66.17
wearing	99.46	riding	93.01
in	90.85	in front of	66.29
near	93.41	standing on	77.84
with	88.20	walking on	90.05
behind	88.72	at	73.19
holding	91.44	attached to	84.01
wears	95.90	belonging to	81.62

The hyper-parameters in our joint loss function Eq. (12) are set as  $\lambda_1 : \lambda_2 : \lambda_3 = 4 : 1 : 1$ .

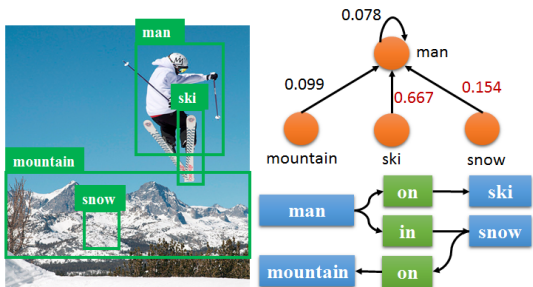


Figure 5. An example of our proposed Graph Self-Attention Module. The top right panel shows the attention weights from other entities to the entity 'man', and the bottom right depicts the ground-truth scene graph.

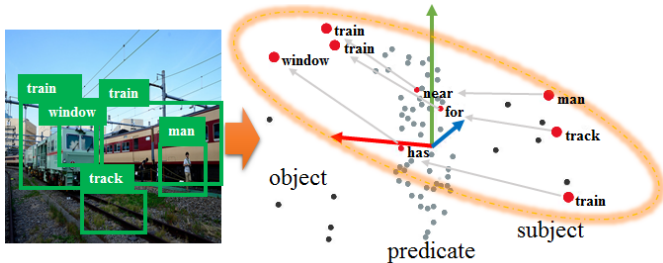


Figure 6. An example of our proposed Semantic Transformation Module. The left is a sample image with its entity bounding boxes visualized. The right is a PCA visualization of entity and relation features in three dimensional space on Scene Graph Classification. The red dots represent detected labels for objects, predicates and subjects.

### 4.3. Quantitative Comparisons

As depicted in Table 1, we compare the performances of our model with the state-of-the-art methods on the Visual Genome. We can see that our model already outperforms all previous methods on the task of SGCLs. For

example, our full model achieves 38.2% and 40.4% w.r.t Recall@50 and Recall@100, which surpass the strong baseline method GPI by about 2% in terms of both metrics. It indicates the superior capability of our model in capturing relations between entity pairs. Semantic transforming linguistic knowledge as well as visual information leads to the best performance on scene graph classification. Moreover, our full model also obtain better performance in terms of PredCls, demonstrating our model’s ability in recognizing relationship accurately. Note that the PredCls task is simply trying to detect predicate which requires less structural information. While our proposed semantic transformation model and graph self-attention module perform best in jointly learning the graph structure. Thus, our model achieves slightly higher accuracy than Neural Motif and GPI. In addition, Table 2 illustrates per-type predicate recall performances of our models on the Visual Genome test set. We find that our model achieve high recall @5 more than 0.85 in most of the frequent predicates, as well as some less frequent predicate, *e.g.* 'walking on' and 'riding' which are harder to learn. We consider the reason is that our framework is able to better modeling contextual information and diverse graph representations to overcome the uneven relationship distribution in the data set.

### 4.4. Ablation Study

We propose Attentive Relational Network which consists two novel modules: *i.e.* semantic transformation module and graph self-attention module. In this subsection, we perform ablation studies to better examine the effect of these two modules.

**Importance of Graph Self-Attention Module:** As shown in Table 1, our model with only Graph Self-Attention Module gain of 2% and 8% compared with Neural Motif and Graph R-CNN, respectively. This improvement can be concluded from the attentive features generated from weighted neighbour embedding. It helps each node to focus on neighbor node features according to context relations. The overall module is thus able to capture more meaningful context across the entire graph to enhance the scene graph generation. Figure 5 illustrates an example of graph self-attention help to generate the scene graph. As can be seen, our model assigns more attention weights from 'ski' to 'man' (0.667) and 'snow' to 'man' (0.154) than 'mountain' to 'man' (0.099), suggesting our proposed module learns to attend more to significant neighbour entities (*e.g.* 'ski' and 'snow'). The ground-truth scene graph demonstrates the detected relationships match the ground truth.

**Importance of Semantic Transformation Module:** By comparing our model with Graph self-Attention and other state-of-the-art methods in Table 1, we notice that our model with only semantic transformation module outperforms all of state-of-the-art methods (*e.g.* Our w/ ST obtain

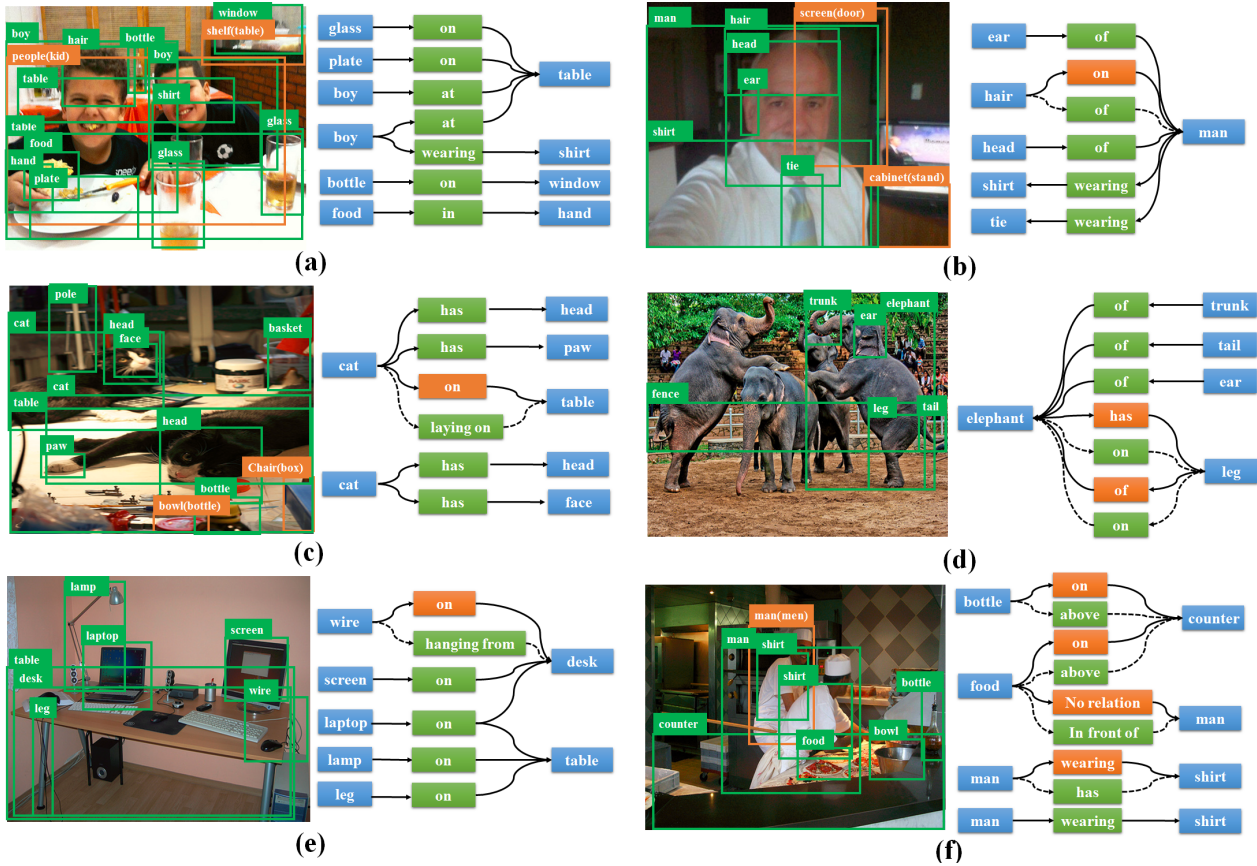


Figure 7. Qualitative results on our proposed Attentive Relational Network. Green and brown bounding boxes are correct and wrong predictions respectively (As for brown labels, our predictions are outside the brackets, while ground truths are inside the brackets). In scene graphs, green and brown cuboids are correct and wrong relation predictions respectively. The dotted lines denote the ground truth relations mistakenly classified by our model. Only predicted boxes that overlap with the ground truth are shown.

37.3% and 40.1% w.r.t Recall@50 and Recall@100 in the task of SGCI on VG). This indicates that the proposed semantic transformation contributes in a significant level to scene graph constructions and visual relationship recognition. Especially, our model with Semantic Transformation only achieves a better result than that of our model with Graph Self-Attention Module only, suggesting that the Semantic Transformation acts as the most important component in our model. By examining the PCA visualization in three dimensional space illustrated in Figure 6, we discovered semantic affinities among the entity type and relation embedding of our module. Meanwhile, we notice apparent clusters of object nodes, predicate nodes and subject nodes in three dimension. Moreover, we find that the existing visual relationship can be translated into a common semantic space (denoted as orange circle in Figure 6), where the entity and relation nodes are connected in an approximate linearity, *e.g.*  $\langle \text{train-has-window} \rangle$ ,  $\langle \text{track-for-train} \rangle$  and  $\langle \text{man-near-train} \rangle$ . It demonstrates that our proposed module can learn semantic knowledge to transform visual feature and word embedding into relation space which benefits

the scene graph generation tasks.

#### 4.5. Qualitative Results

To qualitatively verify the constructed scene graph and visual relations learned by our proposed model, Figure 7 illustrates quite a few visualization examples for scene graph generation on Visual Genome dataset. The results demonstrate that our model is able to semantically predict most of visual relationships in images correctly. As an example, all of visual relationships in the scene graph are correctly detected in Figure 7 (a), which has a complex structure and several different types of objects. Moreover, our model is able to resolve the ambiguity in the object-subject direction. For instance,  $\langle \text{ear-of-man} \rangle$  and  $\langle \text{man-wearing-tie} \rangle$  are predicted correctly by our model in Figure 7 (b). In addition, we observe that our model can predict predicates more accurately than the ground-truth annotations and make more reasonable correct predictions, *e.g.* in Figure 7 (d) and (f) our model outputs  $\langle \text{elephant-has-leg} \rangle$  and  $\langle \text{man-wearing-shirt} \rangle$ , while the ground truth are  $\langle \text{elephant-on-leg} \rangle$  and  $\langle \text{man-has-shirt} \rangle$  that are not inappropriate in the



situation. However, there are still some failure cases in our model. Firstly, some mistakes stem from predicate ambiguity, *e.g.* our model mislead in predicting <bottle-above-counter> and <wire-hanging from-desk> by <bottle-on-counter> and <wire-on-desk> in Figure 7 (f) and (e). Secondly, some mistakes are made due to the failure of the detector. For example, our model can not detect any relation between 'food' and 'man' in Figure 7 (f), and some entities are detected inaccurately, *e.g.* 'door' and 'stand' are misled by 'screen' and 'cabinet' in Figure 7 (b), respectively. Advanced object detection model will be beneficial for improving the performance.

## 5. Conclusion

In this paper, we present a novel *Attentive Relational Network* for scene graph generation. We introduce a semantic transformation module that projects visual features and linguistic knowledge into a common relation space, and a graph self-attention module for joint graph representation embedding. Extensive experiments are conducted on the *Visual Genome Dataset* and our method outperforms the state-of-the-art methods on scene graph generation, which demonstrates the effectiveness of our model. Future works include extending the proposed model to various other tasks such as image captioning and visual question answering.

## References

- [1] B. Alexe, T. Deselaers, and V. Ferrari. Measuring the objectness of image windows. *TPAMI*, 2012.
- [2] Y. Atzmon, J. Berant, V. Kezami, A. Globerson, and G. Chechik. Learning to generalize to new compositions in image understanding. *arXiv preprint arXiv:1608.07639*, 2016.
- [3] A. Bordes, N. Usunier, A. Garcia-Duran, J. Weston, and O. Yakhnenko. Translating embeddings for modeling multi-relational data. In *NIPS*, 2013.
- [4] B. Dai, Y. Zhang, and D. Lin. Detecting visual relationships with deep relational networks. In *CVPR*. IEEE, 2017.
- [5] A. Farhadi, M. Hejrati, M. A. Sadeghi, P. Young, C. Rashtchian, J. Hockenmaier, and D. Forsyth. Every picture tells a story: Generating sentences from images. In *ECCV*. Springer, 2010.
- [6] A. Frome, G. S. Corrado, J. Shlens, S. Bengio, J. Dean, T. Mikolov, et al. Devise: A deep visual-semantic embedding model. In *NIPS*, 2013.
- [7] S. S. Girija. Tensorflow: Large-scale machine learning on heterogeneous distributed systems. 2016.
- [8] R. Herzig, M. Raboh, G. Chechik, J. Berant, and A. Globerson. Mapping images to scene graphs with permutation-invariant structured prediction. *arXiv preprint arXiv:1802.05451*, 2018.
- [9] S. J. Hwang, S. N. Ravi, Z. Tao, H. J. Kim, M. D. Collins, and V. Singh. Tensorize, factorize and regularize: Robust visual relationship learning.
- [10] J. Johnson, R. Krishna, M. Stark, L.-J. Li, D. Shamma, M. Bernstein, and L. Fei-Fei. Image retrieval using scene graphs. In *CVPR*, 2015.
- [11] T. N. Kipf and M. Welling. Semi-supervised classification with graph convolutional networks. *arXiv preprint arXiv:1609.02907*, 2016.
- [12] R. Krishna, I. Chami, M. Bernstein, and L. Fei-Fei. Referring relationships. In *CVPR*, 2018.
- [13] R. Krishna, Y. Zhu, O. Groth, J. Johnson, K. Hata, J. Kravitz, S. Chen, Y. Kalantidis, L.-J. Li, D. A. Shamma, et al. Visual genome: Connecting language and vision using crowdsourced dense image annotations. *IJCV*, 2017.
- [14] S. Lazebnik, C. Schmid, and J. Ponce. Beyond bags of features: Spatial pyramid matching for recognizing natural scene categories. In *null*. IEEE, 2006.
- [15] Y. Li, W. Ouyang, and X. Wang. Vip-cnn: A visual phrase reasoning convolutional neural network for visual relationship detection. *arXiv preprint arXiv:1702.07191*, 2017.
- [16] Y. Li, W. Ouyang, B. Zhou, J. Shi, C. Zhang, and X. Wang. Factorizable net: an efficient subgraph-based framework for scene graph generation. In *ECCV*. Springer, 2018.
- [17] Y. Li, W. Ouyang, B. Zhou, K. Wang, and X. Wang. Scene graph generation from objects, phrases and region captions. In *ICCV*, 2017.
- [18] X. Liang, L. Lee, and E. P. Xing. Deep variation-structured reinforcement learning for visual relationship and attribute detection. In *CVPR*. IEEE, 2017.
- [19] C. Lu, R. Krishna, M. Bernstein, and L. Fei-Fei. Visual relationship detection with language priors. In *ECCV*. Springer, 2016.
- [20] A. Newell and J. Deng. Pixels to graphs by associative embedding. In *NIPS*, 2017.
- [21] A. Newell, Z. Huang, and J. Deng. Associative embedding: End-to-end learning for joint detection and grouping. In *NIPS*, 2017.
- [22] J. Pennington, R. Socher, and C. Manning. Glove: Global vectors for word representation. In *EMNLP*, 2014.
- [23] J. Peyre, I. Laptev, C. Schmid, and J. Sivic. Weakly-supervised learning of visual relations. In *ICCV*, 2017.

- [24] B. A. Plummer, A. Mallya, C. M. Cervantes, J. Hockenmaier, and S. Lazebnik. Phrase localization and visual relationship detection with comprehensive image-language cues. In *CVPR*, 2017.
- [25] M. Qi, J. Qin, A. Li, Y. Wang, J. Luo, and L. Van Gool. stagnet: An attentive semantic rnn for group activity recognition. *ECCV*. Springer, 2018.
- [26] M. Qi, Y. Wang, and A. Li. Online cross-modal scene retrieval by binary representation and semantic graph. In *MM*. ACM, 2017.
- [27] V. Ramanathan, C. Li, J. Deng, W. Han, Z. Li, K. Gu, Y. Song, S. Bengio, C. Rosenberg, and L. Fei-Fei. Learning semantic relationships for better action retrieval in images. In *CVPR*, 2015.
- [28] J. Redmon, S. Divvala, R. Girshick, and A. Farhadi. You only look once: Unified, real-time object detection. In *CVPR*, 2016.
- [29] S. Ren, K. He, R. Girshick, and J. Sun. Faster r-cnn: towards real-time object detection with region proposal networks. *TPAMI*, 2017.
- [30] M. A. Sadeghi and A. Farhadi. Recognition using visual phrases. In *CVPR*. IEEE, 2011.
- [31] K. Simonyan and A. Zisserman. Very deep convolutional networks for large-scale image recognition. *arXiv preprint arXiv:1409.1556*, 2014.
- [32] D. Teney, L. Liu, and A. van den Hengel. Graph-structured representations for visual question answering. *arXiv preprint*, 2017.
- [33] A. Vaswani, N. Shazeer, N. Parmar, J. Uszkoreit, L. Jones, A. N. Gomez, Ł. Kaiser, and I. Polosukhin. Attention is all you need. In *NIPS*, 2017.
- [34] P. Velickovic, G. Cucurull, A. Casanova, A. Romero, P. Lio, and Y. Bengio. Graph attention networks. *arXiv preprint arXiv:1710.10903*, 2017.
- [35] D. Xu, Y. Zhu, C. B. Choy, and L. Fei-Fei. Scene graph generation by iterative message passing. In *CVPR*, 2017.
- [36] J. Yang, J. Lu, S. Lee, D. Batra, and D. Parikh. Graph r-cnn for scene graph generation. *arXiv preprint arXiv:1808.00191*, 2018.
- [37] X. Yang, H. Zhang, and J. Cai. Shuffle-then-assemble: learning object-agnostic visual relationship features. *arXiv preprint arXiv:1808.00171*, 2018.
- [38] T. Yao, Y. Pan, Y. Li, and T. Mei. Exploring visual relationship for image captioning. *arXiv preprint arXiv:1809.07041*, 2018.
- [39] G. Yin, L. Sheng, B. Liu, N. Yu, X. Wang, J. Shao, and C. C. Loy. Zoom-net: Mining deep feature interactions for visual relationship recognition. *arXiv preprint arXiv:1807.04979*, 2018.
- [40] R. Yu, A. Li, V. I. Morariu, and L. S. Davis. Visual relationship detection with internal and external linguistic knowledge distillation. *arXiv preprint arXiv:1707.09423*, 2017.
- [41] R. Zellers, M. Yatskar, S. Thomson, and Y. Choi. Neural motifs: Scene graph parsing with global context. In *CVPR*, 2018.
- [42] H. Zhang, Z. Kyaw, S.-F. Chang, and T.-S. Chua. Visual translation embedding network for visual relation detection. In *CVPR*, 2017.
- [43] H. Zhang, Z. Kyaw, J. Yu, and S.-F. Chang. Ppr-fcn: weakly supervised visual relation detection via parallel pairwise r-fcn. *arXiv preprint arXiv:1708.01956*, 2017.
- [44] H. Zhang, Y. Niu, and S.-F. Chang. Grounding referring expressions in images by variational context. In *CVPR*, 2018.
- [45] J. Zhang, M. Elhoseiny, S. Cohen, W. Chang, and A. Elgammal. Relationship proposal networks. In *CVPR*, 2017.
- [46] B. Zhou, A. Lapedriza, J. Xiao, A. Torralba, and A. Oliva. Learning deep features for scene recognition using places database. In *NIPS*, 2014.
- [47] B. Zhuang, L. Liu, C. Shen, and I. Reid. Towards context-aware interaction recognition for visual relationship detection. In *ICCV*. IEEE, 2017.